**NASA TECHNICAL NOTE**

NASA TN D-5138

# PERFORMANCE AND CAVITATION DAMAGE OF AN AXIAL-FLOW PUMP IN 1500° F (1089 K) LIQUID SODIUM

*by Dean C. Reemsnyder, Walter S. Cunnan, and Carl Weigel*

*Lewis Research Center*
*Cleveland, Ohio*

NATIONAL AERONAUTICS AND SPACE ADMINISTRATION  •  WASHINGTON, D. C.  •  APRIL 1969

# PERFORMANCE AND CAVITATION DAMAGE OF AN AXIAL-FLOW

# PUMP IN 1500° F (1089 K) LIQUID SODIUM

By Dean C. Reemsnyder, Walter S. Cunnan, and Carl Weigel

Lewis Research Center
Cleveland, Ohio

NATIONAL AERONAUTICS AND SPACE ADMINISTRATION

## ABSTRACT

A low-head-rise axial-flow pump was operated in liquid sodium at temperatures to $1500^{\circ}$ F (1089 K) for 558 hr to investigate pump performance and blade cavitation damage in alkali metals. The research rotor had nine insertable blades of three different materials, a blade-tip diffusion factor of 0.40, and a hub-tip-radius ratio of 0.77. Overall performance was obtained, and a 200-hr cavitation endurance test was conducted in $1500^{\circ}$ F (1089 K) sodium at 3450 rpm. Post-test blade inspection indicated that there was slight cavitation damage and that the Ni-Cr-base superalloy (René 41) was more cavitation-damage resistant to high-temperature sodium than either 316 or 318 stainless steel.

ii

# PERFORMANCE AND CAVITATION DAMAGE OF AN AXIAL-FLOW
# PUMP IN 1500° F (1089 K) LIQUID SODIUM

by Dean C. Reemsnyder, Walter S. Cunnan, and Carl Weigel

Lewis Research Center

## SUMMARY

The investigation reported herein concerns pump performance and blade cavitation damage in alkali metals and was conducted in support of condensate pump research for Rankine cycle space electric power systems. A sump-type axial-flow pump was operated for 558 hours in liquid sodium at temperatures to 1500° F (1089 K). The research rotor had nine insertable double circular-arc blades of three different materials, a blade-tip diffusion factor of 0.40, a hub-tip-radius ratio of 0.77, and a blade-tip solidity of 1.0.

Overall pump performance was obtained, and a 200-hour cavitation endurance test was conducted in 1500° F (1089 K) sodium. Cavitation performance tests indicated an initial dropoff in the pump total head-rise coefficient at a suction specific speed of about 6000. This modest suction capability is attributed to the low blade solidity and high hub-tip-radius ratio, which were dictated, respectively, by the requirement of insertable blades and system flow characteristics. The 200-hour pump cavitation endurance test was conducted at a rotational speed of 3450 rpm with a near-design flow coefficient of 0.139 and a head rise 4 percent less than the pump noncavitating head rise. These operating conditions correspond to a suction specific speed of 6500.

Slight blade cavitation damage was concentrated near the tip leading edge of the suction surface. The cavitation damage was apparently caused by the collapse of the vapor generated at the blade tip near the leading edge. The three René 41 (nickel-chromium-base superalloy) blades had less cavitation damage in high-temperature sodium than either the 316 or the 318 stainless-steel blades. All nine blades exhibited an overall surface roughening, which is attributed to corrosion.

# INTRODUCTION

Rankine cycle space power systems utilizing liquid alkali metals, such as potassium or sodium, as the working fluid must operate at high temperature levels. In such systems, vapor generated in the boiler is expanded through a turbine, condensed in the radiator, and returned to the boiler by the condensate pump. Because the fluid is near saturation at the condenser outlet, cavitation in the condensate pump is a problem. Such cavitation may result in a decreased head-producing capability and/or cause damage to the pump impeller. Examples of cavitation damage observed in liquid-metal pumps are illustrated in references 1 to 4. If the overall power system is considered, prevention of pump cavitation by subcooling the condensate is undesirable because it would require a substantial increase in the radiator area.

Visual studies of cavitation indicate that vaporous regions can exist in the pump impeller at inlet pressures substantially greater than that at which performance degradation occurs (ref. 5). The extent of these vaporous regions increases as the inlet pressure is decreased, eventually resulting in a reduction in pump head rise. Because of the unusually low inlet pressure, condensate pumps may be required to operate with cavitation present in the impeller while maintaining a good head-rise-producing capability.

Since cavitation may be present in the condensate pump impeller, it must be fabricated from materials that exhibit suitable mechanical and chemical resistance characteristics in the high-temperature liquid metals. Resistance of a number of materials to cavitation damage has been examined (ref. 6) by utilizing a magnetostrictive vibrator device in $800^{\circ}$ F (700 K) sodium. Stainless steels 316 and 318 exhibited reasonably good resistance to cavitation damage, but René 41 showed an even greater resistance. Thus, these three materials are representative of those that may be suitable for the fabrication of liquid-metal pump impellers.

The objectives of this investigation were to determine the extent of long-term cavitation damage that may be expected to occur in a pump-inlet-stage rotor in $1500^{\circ}$ F (1089 K) liquid sodium and to evaluate the relative resistance to cavitation damage of three representative rotor blade materials, 316 and 318 stainless steel and René 41, a nickel (Ni)-chromium (Cr)-base superalloy. A 5.0-inch- (127-mm-) diameter axial-flow rotor was designed so that blades of these three materials could be inserted in the rotor. The performance of the pump was evaluated for both cavitating and noncavitating operation. Operating conditions for the endurance test were selected by considering the effect of inlet pressure on the pump performance. The pump was operated under cavitation conditions in $1500^{\circ}$ F (1089 K) sodium at a rotational speed of 3450 rpm for 200 hours during the cavitation endurance test. Subsequent cavitation studies were made in water to observe the cavitation vapor formations that probably existed at the operating conditions for the endurance test.

# PUMP ROTOR DESIGN

The test rotor was designed, built, and tested (1) to determine the role of damaging cavitation vapor on the blade surface and (2) to establish the relative resistance to this damage of three rotor blade materials.

## Blade Design

Cavitating inducers are capable of adding energy to the fluid even when cavitation exists within the inducer. High inlet flow angles ($> 80°$) are usually required to obtain the high suction specific speeds normally associated with inducers. In the present design, an inlet tip flow angle of $81.3°$ with respect to the rotor axis was used. Thus, with cavitation in the blade passages, the resulting vapor formation and cavitation damage could be expected to be representative of that encountered with inducers of conventional design. Conventional inducers with long thin blades are not particularly well suited for a cavitation-damage study to determine the relative resistance of various blade materials. Consequently, for ease of fabrication and simultaneous testing of various blade materials, the rotor design chosen incorporated nine individually insertable blades. However, this design limited the blade chord, which resulted in a blade-tip solidity of 1.0. Also, flow rate and other limitations of the existing sodium test facility restricted the rotor hub-tip-radius ratio to a relatively high value of 0.77. Although it was anticipated that these constraints limit the suction performance, the rotor design was considered a reasonable compromise to obtain cavitation-damage characteristics of a cavitating inducer in liquid sodium.

In addition to the aforementioned considerations, the rotor design included the following assumptions: constant inlet absolute axial fluid velocity, constant energy addition at all blade radii, simplified radial equilibrium, and constant blade efficiency (actual head rise/ideal head rise) at each section. The blade-hub and tip-diffusion factors were 0.6 and 0.4, respectively. The design procedure followed that presented in references 7 and 8 and utilized design information from reference 9. Rotor design values were as follows:

Fluid inlet temperature, $°F$; K . . . . . . . . . . . . . . . . . . . . . . . . . . . . . 1500; 1089
Flow rate, Q, gal/min; cu m/sec . . . . . . . . . . . . . . . . . . . . . . 280; 0.0177
Rotative speed, N, rpm . . . . . . . . . . . . . . . . . . . . . . . . . . . . . . . . . 3450
Flow coefficient, $\varphi$ . . . . . . . . . . . . . . . . . . . . . . . . . . . . . . . . . 0.147
Head-rise coefficient, $\psi$ . . . . . . . . . . . . . . . . . . . . . . . . . . . . . . 0.20

The rotor blade design parameters at room temperature are given in table I. The tip diameter increases about 0.075 inch (1.90 mm) from room temperature to $1500^{\circ}$ F (1089 K). The operating tip clearance of about 0.033 inch (0.84 mm) remains relatively constant because the thermal coefficients of expansion are about the same for the blade materials and the 316 stainless-steel housing and hub. Mechanical design limitations involved in operating the pump in high-temperature sodium prevented the use of a smaller tip clearance.

Double circular-arc blade sections were selected to obtain thin leading edges, which are desirable for good cavitation performance. The leading and trailing edges were machined to 0.010-inch (0.254-mm) radii. A schematic drawing of the rotor blades along with the inlet and outlet vector diagrams are shown in figure 1. The design tip fluid turning angle was $3^{\circ}$, which was attained by setting a $4^{\circ}$ cambered section for an incidence angle of $2.8^{\circ}$ and a deviation angle of $3.8^{\circ}$.

TABLE I. - BLADE DESIGN PARAMETERS

OF AXIAL-FLOW ROTOR

| | |
|---|---|
| Rotor geometry | |
| Tip diameter, in. (mm) | 4.956 (126.0) |
| Hub-tip-radius ratio | 0.77 |
| Number of blades | 9 |
| Blade-tip radial clearance, in. (mm) | 0.033 (0.84) |
| Leading and trailing edge radii, in. (mm) | 0.010 (0.254) |
| | |
| Tip geometry (double circular-arc sections) | |
| Solidity, $\sigma_t$ | 1.00 |
| Diffusion factor, $D_t$ | 0.40 |
| Chord length, c, in. (mm) | 1.743 (44.3) |
| Ratio of maximum thickness to chord | 0.06 |
| Stagger angle with respect to axis, deg | 76.5 |
| Camber angle, deg | 4.0 |
| Incidence angle, $i_t$, deg | 2.8 |
| Deviation angle, $\delta_t$, deg | 3.8 |
| Inlet blade angle, $\kappa_{1,t}$, deg | 78.5 |
| | |
| Hub geometry (double circular-arc sections) | |
| Solidity, $\sigma_h$ | 1.30 |
| Diffusion factor, $D_h$ | 0.60 |
| Chord length, c, in. (mm) | 1.743 (44.3) |
| Ratio of maximum thickness to chord | 0.08 |
| Stagger angle with respect to axis, deg | 70.5 |
| Camber angle, deg | 19.4 |
| Incidence angle, $i_h$, deg | -1.7 |
| Deviation angle, $\delta_h$, deg | 8.9 |
| Inlet blade angle, $\kappa_{1,h}$, deg | 81.0 |
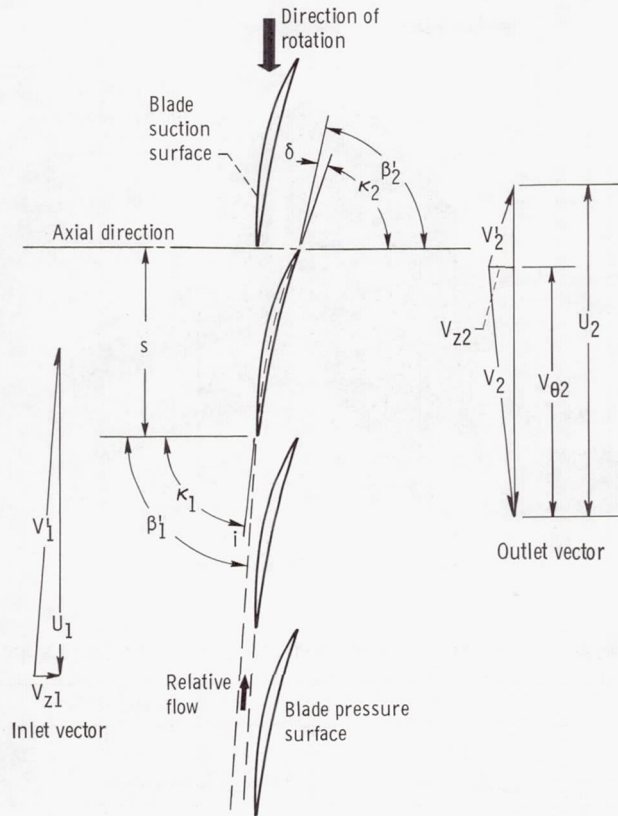
Figure 1. - Blade nomenclature and vector diagrams.

## Blade Material Considerations

The resistance to cavitation damage in liquid sodium was the major consideration in the selection of blade materials. Since material damage resistance is a measure of the capacity of a material to withstand the high local stresses caused by the collapsing bubbles, high values of yield strength, ultimate tensile strength, and ductility (elongation) are desirable to provide resistance to cavitation damage. Available information indicates that 316 stainless steel has relatively good cavitation-damage resistance to high-temperature liquid sodium (ref. 10). Two other blade materials, 318 stainless steel and René 41 (a Ni-Cr-base superalloy), were also selected on the basis of their properties of high-temperature strength and corrosion resistance at $1500^\circ$ F (1089 K). Some significant properties of each selected blade material at $1500^\circ$ F (1089 K) are presented in table II.

The nine blades (three each of the three different materials) were installed in slots and held by close-fitting pins in the test rotor shown in figure 2. The three blades of each material are equally spaced (i.e., at $120^\circ$ intervals) around the hub.
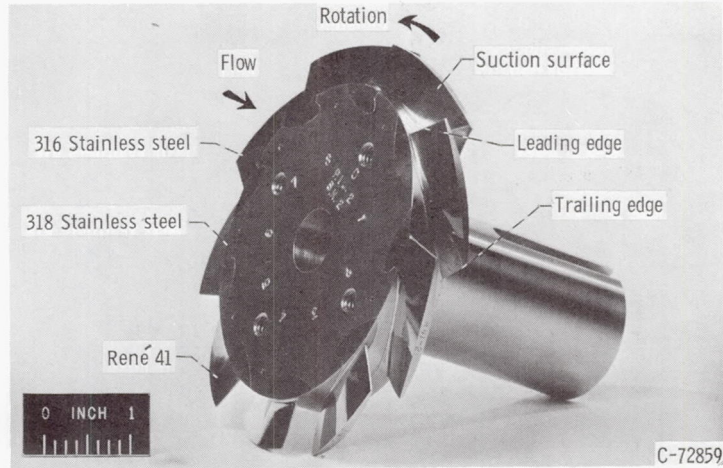
Figure 2. - Axial-flow rotor before test.

TABLE II. - SOME PHYSICAL PROPERTIES OF ROTOR BLADE MATERIALS AT 1500° F (1089 K)[a]

| Property | Material | | |
|---|---|---|---|
| | A.I.S.I. 316 Stainless steel | A.I.S.I. 318 Stainless steel | Haynes alloy R-41 René 41 |
| Ultimate tensile strength, psi $(N/m^2)$ | 31 000 $(220 \times 10^6)$ | 31 000 $(220 \times 10^6)$ | 126 000 to 130 000 $(869 \times 10^6$ to $895 \times 10^6)$ |
| Yield strength, psi $(N/m^2)$ | 20 000 $(138 \times 10^6)$ | 15 000 $(103 \times 10^6)$ | 110 000 to 118 000 $(758 \times 10^6$ to $813 \times 10^6)$ |
| Elongation, percent | 40 | 40 | 5 to 14 |
| Coefficient of thermal expansion from 70° to 1600° F (294 to 1144 K), in./(in.)(°F) (m/(m)(K)) | $10.8 \times 10^{-6}$ $(19.42 \times 10^{-6})$ | ------ | $8.7 \times 10^{-6}$ $(15.65 \times 10^{-6})$ |

[a]Refs. 11 and 12.

# APPARATUS AND PROCEDURE

## Pump Assembly

A drawing of the sump-type pump assembly is presented in figure 3. The pump consists of a stationary inlet nose piece, an axial-flow rotor, a stationary outlet vaneless diffuser, and a collector. The Inconel collector is welded to the expansion tank, which also acts as a fluid reservoir or sump. The inlet assembly is stationary and forms an annular flow passage to the rotor. Sodium internal leakage flows from the pump outlet through the clearance in the outlet transition piece to the expansion tank. A small amount of sodium also flows up the shaft and through the triple-threaded screw-type shaft seal to the expansion tank.
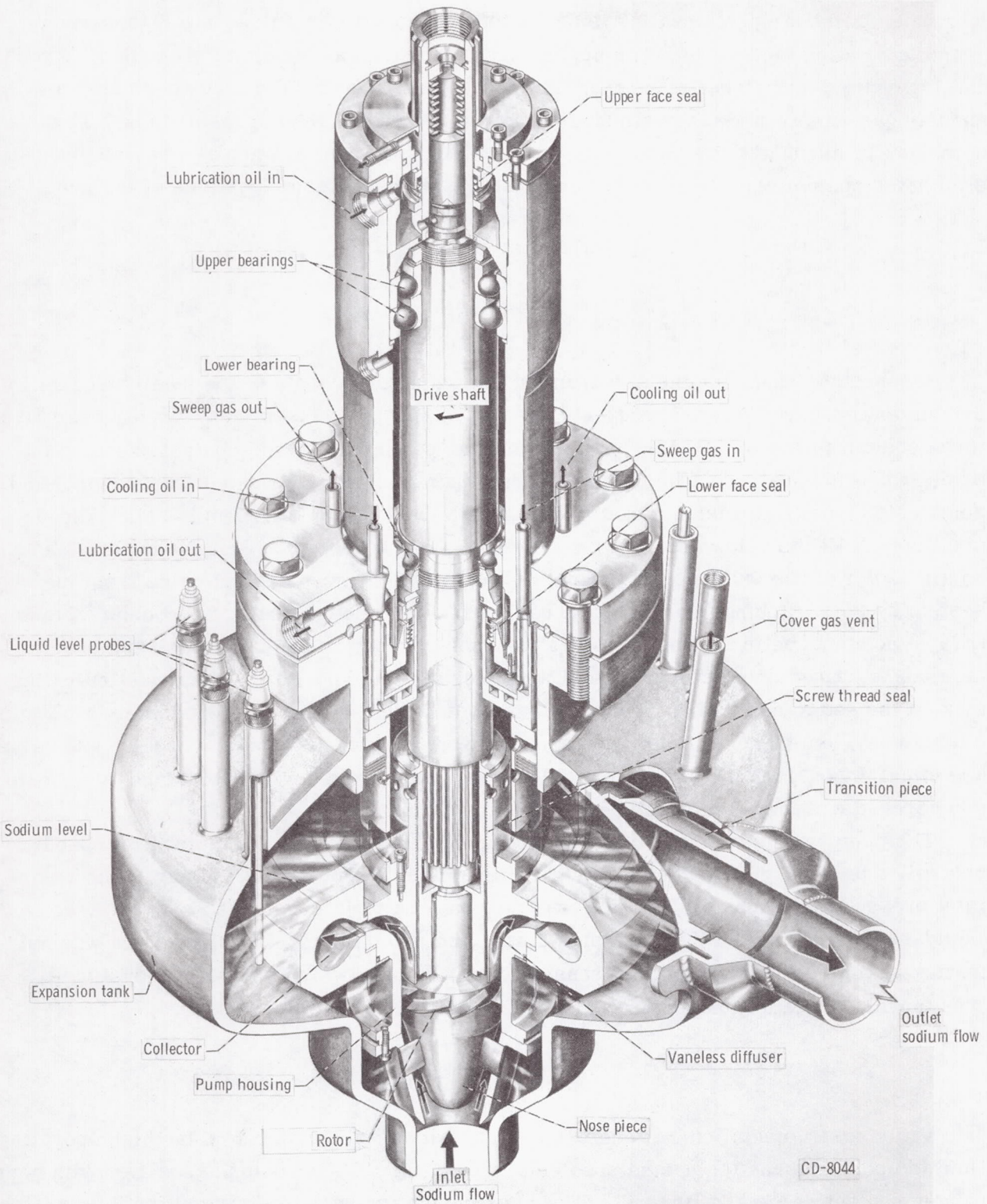
Figure 3. - Sodium pump assembly.

Upper face seal

Lubrication oil in

Upper bearings

Lower bearing

Sweep gas out

Cooling oil in

Lubrication oil out

Liquid level probes

Sodium level

Expansion tank

Collector

Pump housing

Rotor

Drive shaft

Cooling oil out

Sweep gas in

Lower face seal

Cover gas vent

Screw thread seal

Transition piece

Outlet sodium flow

Vaneless diffuser

Nose piece

Inlet Sodium flow

CD-8044

The pump drive shaft is mounted vertically and is supported by angular-contact oil-lubricated ball bearings. Sealing is accomplished with two stainless-steel-to-carbon-graphite rotating face seals. The upper part of the pump assembly is oil cooled. Argon gas is supplied to the area around the lower face seal, flows down a close-clearance annular passage around the pump shaft, and is vented from the expansion tank. This down flow of argon gas prevents sodium-vapor migration up the annular passage and thus eliminates sodium deposition on the lower seal and on the cooler portions of the pump shaft.
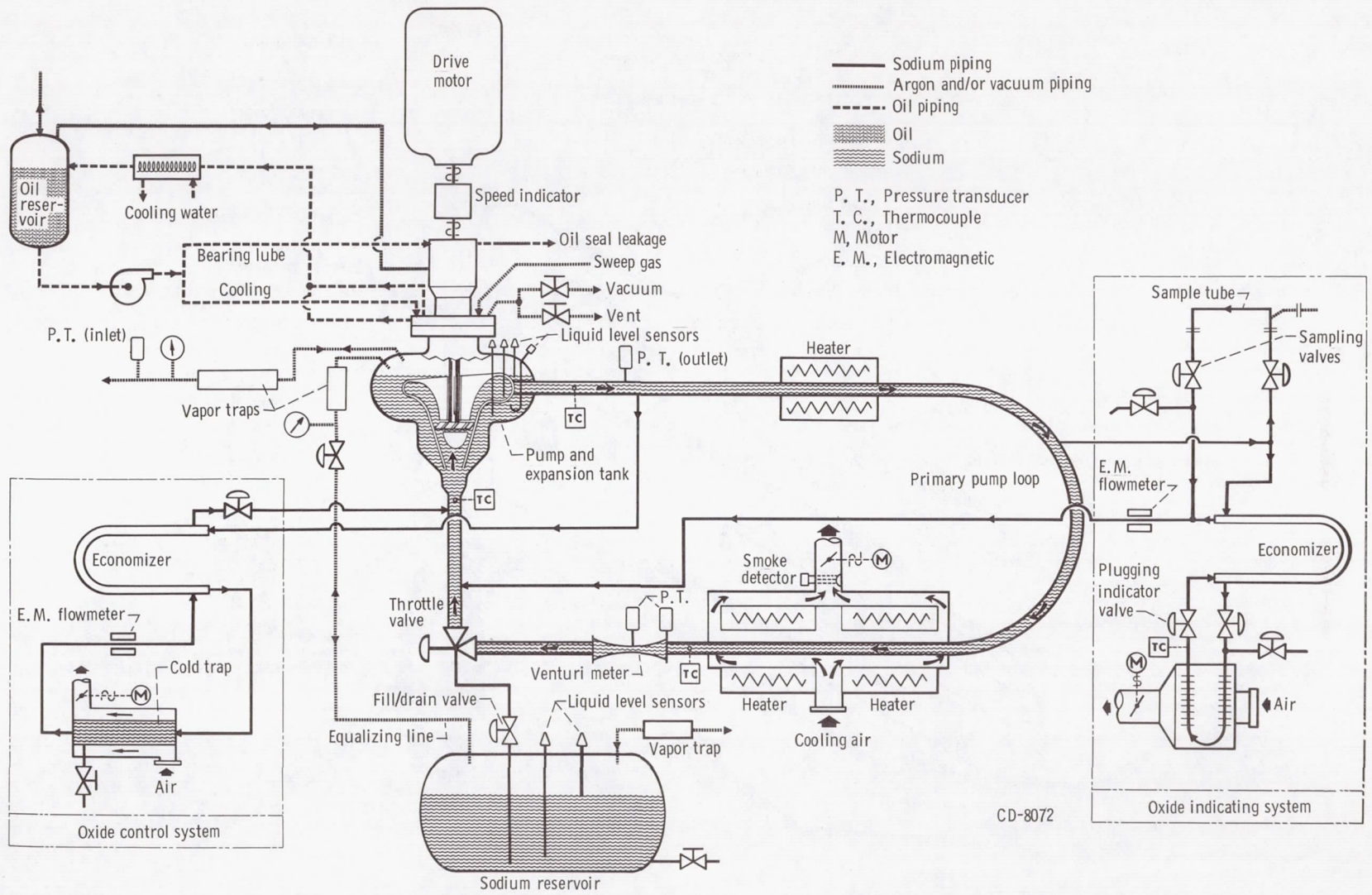
## Test Facility

A schematic diagram and a drawing of the main components of the pump test facility are shown in figures 4 and 5, respectively. The alkali-metal pump test facility comprises three sodium process systems: primary sodium pump loop, oxide control system, and oxide indicating system. The primary sodium pump loop is fabricated from Inconel and contains the pump expansion tank and test pump, the 4-inch- (101.7-mm-) schedule-40 pipe loop, a Venturi flowmeter, a throttle valve, three split-tube electric heaters, and an air cooler. The oxide control system, designed to remove sodium oxide from the system by cold trapping, consists of a concentric-tube heat exchanger (economizer), cold trap, electromagnetic flowmeter, and a flow control valve. Sodium oxides are precipitated and retained on a stainless-steel wire mesh in the cold trap. The oxide indicating system is used to determine the concentration of sodium oxide in the system by a plugging indicator system and a sampling system. All sodium process piping, vessels, and valves are either Inconel or 316 stainless steel and are trace heated with resistance-type heaters and covered with high-temperature thermal insulation.

The pump was driven by a 100-horsepower (74.6-kW) induction motor at a speed controlled between 600 and 3450 rpm by a variable-frequency power supply. The pump inlet pressure was controlled by pressurizing with an inert cover gas above the free liquid-sodium surface in the expansion tank. The pump inlet fluid temperature was automatically controlled to maintain a constant temperature, which was sensed by a well-type thermocouple located at the centerline of the pump inlet pipe.
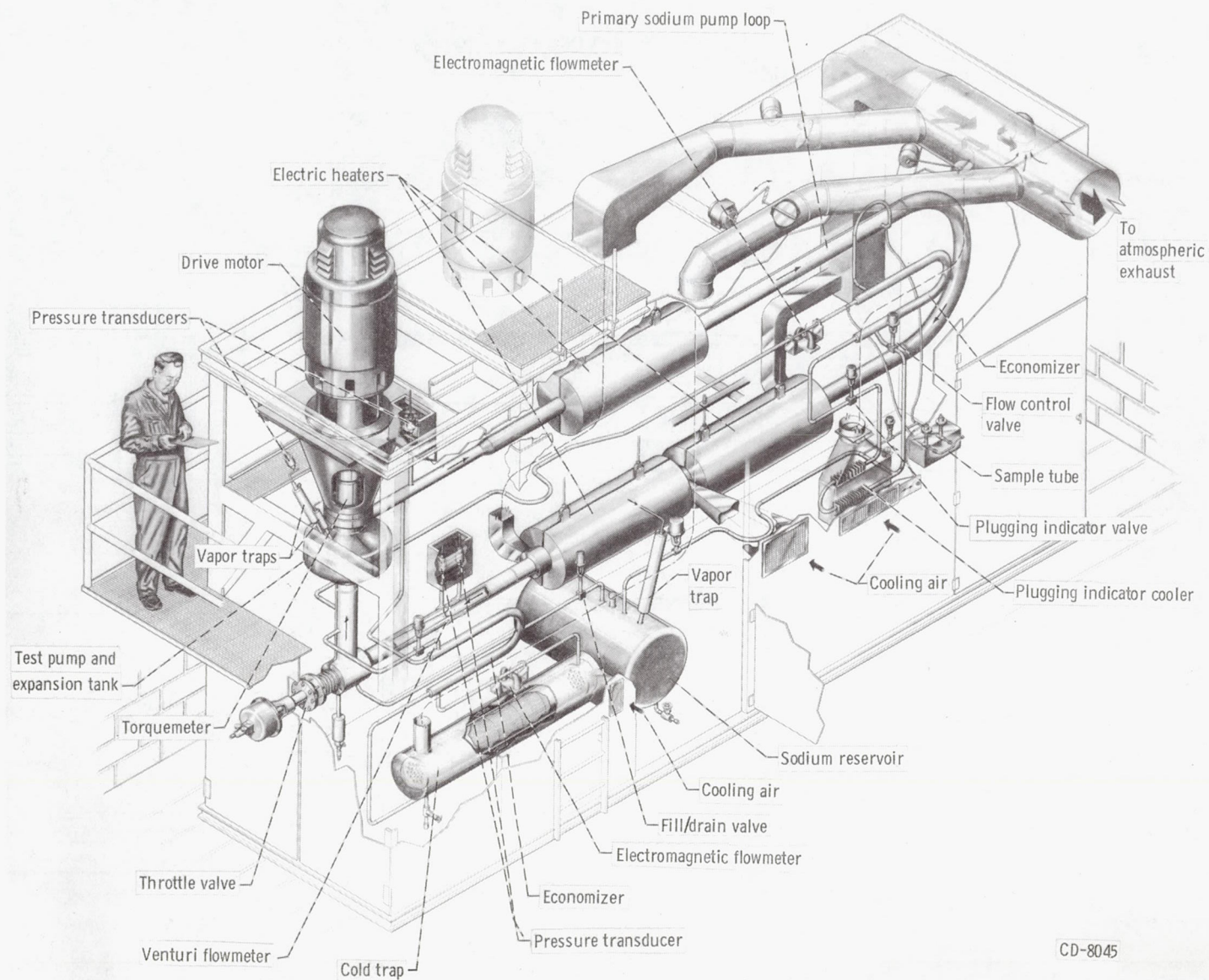
## Instrumentation

Major instrumentation considerations in alkali-metal systems are the high operating fluid temperature and the unique problems of plugging and corrosion associated with high oxygen content in the alkali metal. The instrumentation systems utilized for this test are described in the following sections.

Figure 4. - Alkali-metal pump test facility.

Drive motor

Speed indicator

Oil seal leakage
Sweep gas
Vacuum
Vent
Liquid level sensors

Oil reservoir

Cooling water

Bearing lube
Cooling

P. T. (inlet)

Vapor traps

P. T. (outlet)

Heater

Pump and expansion tank

Primary pump loop

Smoke detector

Throttle valve

Venturi meter

Fill/drain valve

Liquid level sensors

Equalizing line

Vapor trap

Heater    Heater

Cooling air

Economizer

E.M. flowmeter

Cold trap

Air

Oxide control system

Sodium reservoir

CD-8072

Sample tube

Sampling valves

E. M. flowmeter

Economizer

Plugging indicator valve

Air

Oxide indicating system

——— Sodium piping
·········· Argon and/or vacuum piping
- - - - - Oil piping
▨ Oil
≈ Sodium

P. T., Pressure transducer
T. C., Thermocouple
M, Motor
E. M., Electromagnetic

Figure 5. - Alkali-metal pump test facility showing relative size.

Pressure. - Four unbonded-wire-strain-gage-type absolute-pressure transducers and one precision evacuated-bellows-type absolute-pressure gage were utilized to determine system static pressures. Transducers sensed the static pressure directly in the pump outlet line and in the Venturi flowmeter inlet and throat locations (fig. 4). These transducers were thermally isolated from the fluid by argon gas in the vertical pressure lines. Temperature control of the pressure transducer lines ensured that the sodium was maintained above its oxide plugging temperature. The transducers were immersed in constant-temperature oil baths automatically controlled at $225^O$ F (380 K). A transducer, mounted on the expansion tank, sensed argon cover-gas (pump-inlet) pressure through a vapor trap and was exposed to $125^O$ F (325 K) ambient air. An absolute-pressure gage was also used to monitor expansion-tank cover-gas pressure.

Flow. - The sodium flow of the primary system was determined by an air-calibrated Venturi flowmeter (room-temperature throat diam of 1.680 in. or 42.6 mm). Electromagnetic flowmeters measured the flows of the oxide control and oxide indicating systems, the flow of each being less than 1 percent of the research pump flow. Pump flow is rotor flow less internal leakage. This leakage was not measured but was computed to be 3 to 10 percent of the total flow over the pump operating range.

Temperature. - Thermocouples used to measure the pump inlet and outlet and the Venturi inlet temperatures were fabricated from calibrated Chromel-Alumel thermocouple wire. These spring-loaded open-ball thermocouples were installed in pipe wells located approximately at the system pipe centerline. A heated reference-junction box was thermostatically controlled at $150\pm0.25^O$ F ($339\pm0.14$ K) for all the thermocouples connected to the digital voltmeter.

Liquid level. - The sodium liquid level in the expansion tank was sensed continuously by a resistance-type J-probe powered by a 6-volt alternating-current signal.

Speed. - The pump speed was sensed by a magnetic pickup located on the pump shaft and was indicated on an electronic counter.

## Test Procedure

The sodium pump test program consisted of two parts. First, both cavitating and noncavitating pump performance were obtained. Then a 200-hour cavitation endurance test was conducted at a head dropoff of approximately 4 percent of the noncavitating head. The throttle valve setting was not changed during the endurance test, and both the pump speed and pump inlet temperatures were automatically controlled at the set point. Minor manual adjustments of the pump sweep gas and vent flows were required to maintain the pump inlet pressure constant. The oxygen content of the sodium was maintained at or below 50 parts per million by weight. Measurements were recorded hourly during the 200-hour endurance test.

Experimental data were reduced and corrected to account for instrument calibrations, the thermal expansion of pump parts and Venturi flowmeter, a change in sodium fluid properties as a function of temperature, hydrostatic heads in the expansion tank and pressure transducer lines, a change in the Venturi flowmeter coefficient of discharge with throat Reynolds number, and oxide control and indicating system flows that bypassed the Venturi flowmeter. Velocity heads were computed based on flow and area considerations and were added to the measured static heads to obtain total heads. The net positive suction head $H_{sv}$ was calculated from the inlet total pressure minus the vapor pressure corresponding to the fluid inlet temperature. The pump total head rise was obtained from the measurement of expansion-tank pressure (inlet pressure) and pump outlet-line static pressure and adjusted for the computed velocity and hydrostatic heads. The pump total head rise is the rotor head rise minus the head losses in the pump inlet, stationary outlet diffuser, and volute collector.

The estimated experimental precision of pertinent test measurements and pump performance parameters at a design flow of approximately 264 gallons per minute (0.0167 cu m/sec) are presented in table III.

TABLE III. - EXPERIMENTAL PRECISION

[Design flow rate, Q, 264 gal/min (0.0167 cu m/sec).]

| Parameter | Precision |
|---|---|
| Fluid | |
| Temperature, $^O$F (K) | ±10 (±5.6) |
| Density, $\rho$, (lb)(sec$^2$)/ft$^4$ ((N)(sec$^2$)/m$^4$) | ±0.004 (±2.1) |
| Static pressures, psi (N/m$^2$): | |
| Pump inlet, $p_1$ | ±0.03 (±205) |
| Pump outlet, $p_2$ | ±0.13 (±900) |
| Venturi differential | ±0.19 (±1300) |
| | |
| Pump | |
| Rotative speed, N, rpm | ±2 |
| Flow rate, Q, gal/min (cu m/sec) | ±6.7 (4.2×10$^{-4}$) |
| Total head rise, ΔH, ft (m) | ±0.9 (±0.3) |
| Net positive suction head, $H_{sv}$, ft (m) | ±1.6 (±0.5) |
| Suction specific speed, $S_s$ | ±525 |
| Flow coefficient, $\varphi$ | ±0.004 |
| Head-rise coefficient, $\psi$ | ±0.005 |

# RESULTS AND DISCUSSION

The axial-flow pump was operated for 558 hours in liquid sodium. Initial cold trapping to remove sodium oxide was accomplished at a system temperature of $1000^{\circ}$ F (810 K). This procedure was followed by 405 hours of test operation at $1500^{\circ}$ F (1089 K), which included a 200-hour endurance test under cavitating flow conditions.

Pump cavitation performance (and noncavitating performance for comparison) is presented in nondimensional terms in figure 6 for various values of net positive suction head. All data were obtained at a rotative speed of 3450 rpm and a sodium temperature of $1500^{\circ}$ F (1089 K). Blade-tip speed was 75.5 feet per second (23.0 m/sec). The characteristic noncavitating performance curve of the head-rise coefficient $\psi$ as a function of the flow coefficient $\varphi$ in figure 6 shows the nearly linear relation typical of an axial-flow inducer. Overall pump performance was probably adversely affected by
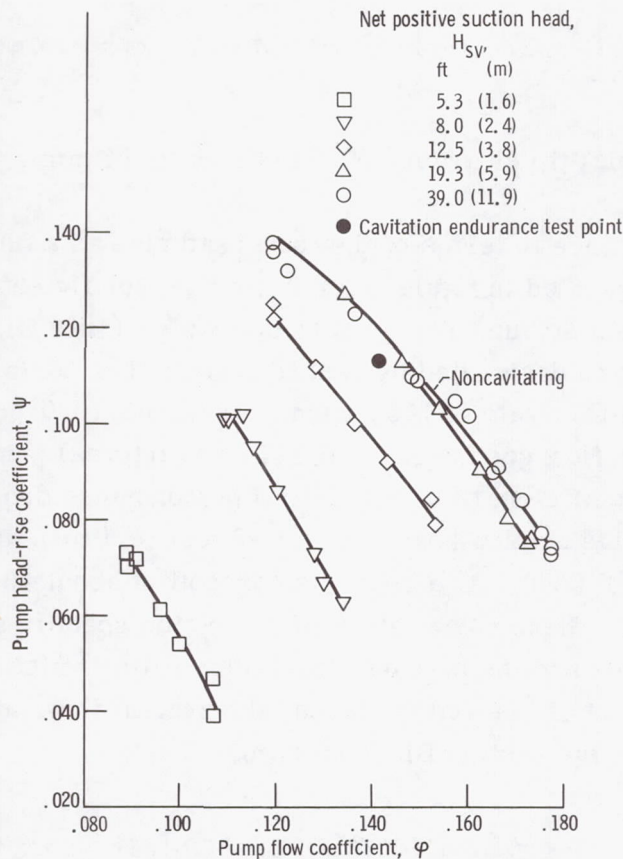


Figure 6. - Pump cavitation performance in $1500^{\circ}$ F (1089 K) sodium at 3450 rpm and several values of net positive suction head.
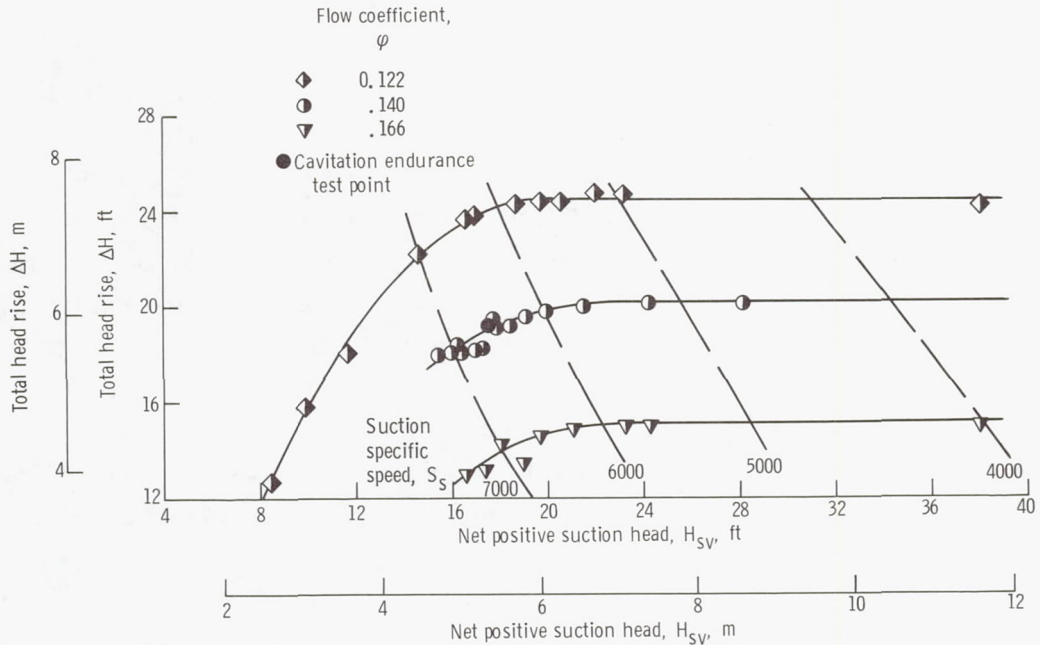
Figure 7. - Pump cavitation performance in 1500° F (1089 K) sodium at 3450 rpm and three flow coefficients.

the relatively large radial tip clearance of 0.033 inch (0.84 mm), which is 6 percent of the blade height.

Cavitation performance in terms of the total head rise as a function of the net positive suction head is presented in figure 7 for three flow coefficients, a constant rotative speed of 3450 rpm, and a sodium temperature of 1500° F (1089 K). (Curves of constant suction specific speed are designated by dashed lines.) The pump flow coefficient of 0.140 corresponds to a flow rate of 266 gallons per minute (0.0168 cu m/sec) and approximates the rotor design flow coefficient of 0.147 when internal pump leakage is considered. At the flow coefficient of 0.140, initial performance dropoff due to cavitation occurred at a net positive suction head of about 20 feet (6.1 m), which corresponds to a suction specific speed of 6000. At a head-rise dropoff of about 10 percent, the suction specific speed is 7000. These relatively modest suction specific speeds are attributed to the short blade chords and the high hub-tip-radius ratio, which were dictated respectively by the requirement of insertable blades, the system flow, and the geometric limitations (as discussed in the section Blade Design).

## Cavitation Endurance Test

After the pump performance was established, a continuous 200-hour cavitation endurance test was conducted in 1500° F (1089 K) sodium at approximately design flow.

14

TABLE IV. - CAVITATION ENDURANCE TEST PARAMETERS

|  | Nominal value | Standard deviation |
|---|---|---|
| Fluid inlet temperature, $^{o}F$ (K) | 1509 (1092) | ±3.3 (±1.8) |
| Rotative speed, N, rpm | 3442 | ±10 |
| Pump flow rate, Q, gal/min (cu m/sec) | 264 (0.0167) | ±1.3 (±8.2×10$^{-5}$) |
| Pump total head rise, ΔH, ft (m) | 19.5 (6.0) | ±0.2 (0.06) |
| Flow coefficient, $\varphi$ | 0.139 | ±0.001 |
| Head-rise coefficient, $\psi$ | 0.110 | ±0.001 |
| Net positive suction head, $H_{sv}$, ft (m) | 17.6 (5.4) | ±0.4 (±0.12) |
| Suction specific speed, $S_s$ | 6500 | ±120 |

The endurance operating point was selected to give a 4-percent dropoff from the pump noncavitating head rise (figs. 6 and 7). Nominal values of the significant pump performance and cavitation parameters for the 200-hour endurance test and the calculated standard deviation from these nominal or mean values are tabulated in table IV. No deterioration in pump performance was observed during the test. The blade-tip speed was about 75 feet per second (22.8 m/sec), and the nominal value of suction specific speed for the 200-hour endurance test was 6500. The average relative fluid velocity at the inlet blade tip was 76.4 feet per second (23.2 m/sec).

## Photographs of Rotor Cavitation Formations in Water

For observation of the rotor cavitation patterns that probably existed during the sodium endurance test, an identical rotor (except for direction of rotation) was tested in room-temperature water in a water tunnel at the NASA Lewis Research Center. A transparent window in the housing permitted both visual observation and photographing of the rotor cavitation patterns in the room-temperature deaerated water (gas content, < 3 ppm by weight). The visual observations were made with a stroboscopic light source that was synchronized with the pump shaft. The photographs were taken with a 70-millimeter camera that was synchronized with a high-intensity, short-duration light source for use in high-speed stop-motion photography.

Photographs of the cavitation formations in water are shown in figure 8. The flow coefficient (0.143) and rotative speed (3450 rpm) for the water test were approximately the same as those for the sodium endurance test. These photographs indicate increasing amounts of vapor with a decreasing net positive suction head. The vapor is largely con-
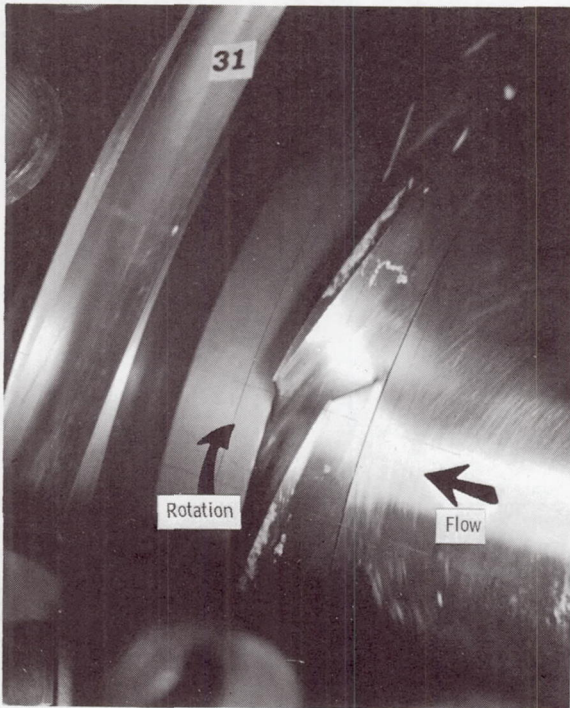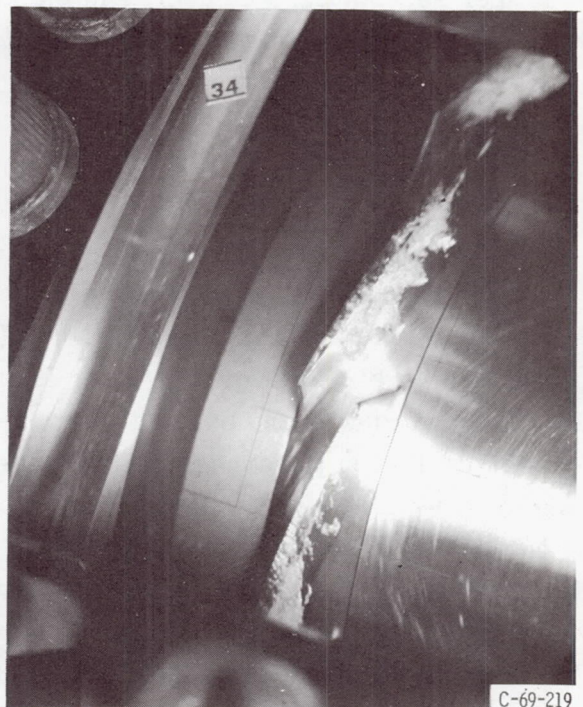
(a) Net positive suction head, 34.3 feet (10.5 m); suction specific
speed, 4000.
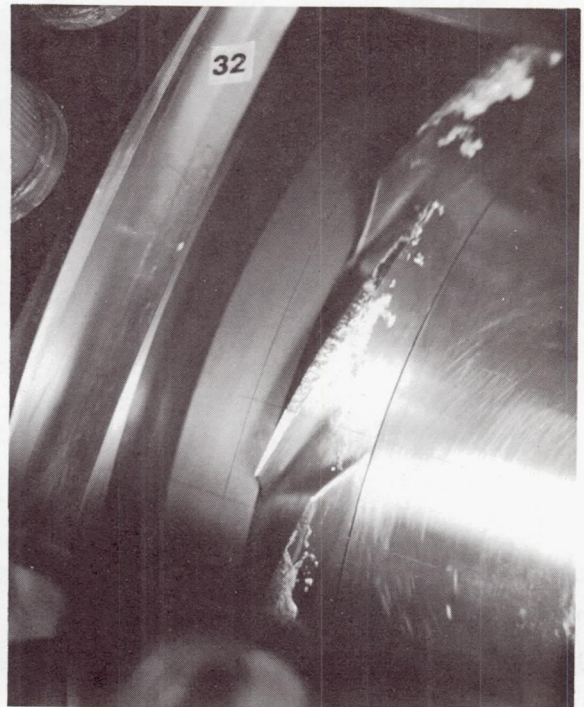
(b) Net positive suction head, 19.8 feet (6.0 m); suction specific
speed, 6000.

(c) Net positive suction head, 17.8 feet (5.4 m); suction specific
speed, 6500.

(d) Net positive suction head, 14.8 feet (4.5 m); suction specific
speed, 7500.

Figure 8. – Rotor cavitation formation in 80° F (300 K) water at 3450 rpm and flow coefficient of 0.143.

fined to the region near the rotor tip and is generated by high velocities in the tip vortex. This tip cavitation is caused by the interaction between the main stream through flow and the cross flow through the blade-tip clearance space.

The photograph of figure 8(c) was taken at approximately the same flow coefficient, rotative speed, and net positive suction head as those for the sodium cavitation endurance test. In this figure, a small amount of vapor can be seen near the blade tip and leading edge on the suction surface of the middle blade. Visual observation of the operating rotor revealed that this vapor formed and collapsed in an irregular manner. Also, the tip vortex cavitation appeared to be confined to the flow channel because it did not cross the channel to impinge on the following blade.

## Rotor Blade Damage in Sodium

The mechanism involved in cavitation damage to materials is generally considered to result from the exposure of the material to the jet impingement and pressure shock waves of imploding bubbles on or very near its surface (ref. 10). Damage resistance, then, is a measure of the capacity of a material to absorb this mechanical attack before fracture or pitting occurs. The mechanism of cavitation damage is very complex and involves hydrodynamic and metallurgical variables, and, in corrosive media, chemical and electrochemical effects as well.

Following the sodium endurance test, the blades were inspected for cavitation damage. A post-test photograph of the rotor showing the suction surfaces of three blades is presented in figure 9. Suction surface damage consisted of a few random pits except for an area near the blade-tip leading edge where damage was more severe (dashed outline on blade 9, fig. 9). Enlarged photographs of this area for the most severely damaged blade of each material are shown in figure 10. The white areas evident in figures 9 and 10 are residual sodium oxide. A comparison of the pretest photograph (fig. 10(a)) with the post-test photograph of blade 9 (fig. 10(b)) indicates a roughening of the blade surface that resulted from corrosion.

The area where locally concentrated cavitation damage occurred was on the suction surface of the blade near the tip (fig. 10(c)). The damage area was elliptical in shape and was about 1/8 inch (3.18 mm), in chord direction, by about 0.040 inch (1.0 mm), in radial direction. The damage was apparently caused by the collapse of the vapor generated near the tip and leading edge of the blade. These vapor formations can be observed in the water photographs of figure 8(c) that were taken at conditions corresponding to the sodium cavitation endurance test.

René 41 was the most resistant of the three materials tested because it sustained the least amount of damage (fig. 10(d)). Damage evaluations of all nine blades indicated that
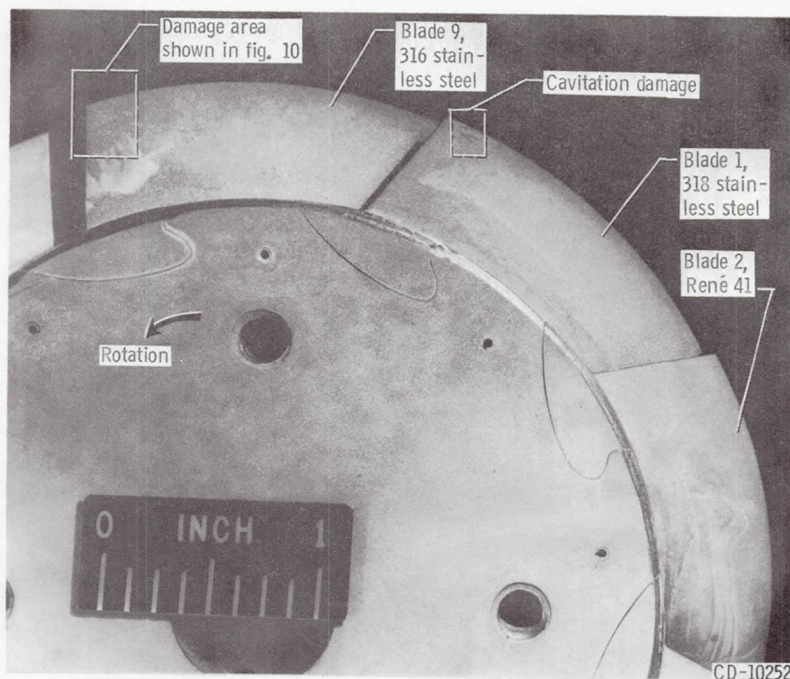
Figure 9. - Post-test suction surface of three rotor blades. (White areas are residual sodium oxide.)

both 316 and 318 stainless steel sustained about the same amount of cavitation damage. The same three materials were tested in sodium with a magnetostrictive device and similar comparative results were obtained (ref. 6).

Damage on the blade pressure surface was minor and consisted of a few random pits near the blade trailing edge. These pits may have been generated during the performance tests in which the rotor was operated over a range of flows and inlet pressures. As discussed in the section Photographs of Rotor Cavitation Formations in Water, the photograph of the cavitation vapor distribution taken in water (fig. 8(c)) indicates that, at the conditions of the endurance test, the tip vortex cavitation formation was confined to the channel between blades and did not cross the channel to cause pressure surface damage to the following blade.

Surface roughening, which was observed over the entire surface of all blades, is attributed to corrosion attack by the high-temperature sodium. The corrosion attack may have been accelerated by the relatively high oxide content (above 50 ppm) during the initial cold-trapping operation at $1000^{\circ}$ F (810 K). Post-test photomicrographs were taken of undamaged sections through three blade tips. The general surface profile is presented in figure 11. Surface roughening occurred to depths of about 0.001 inch (0.025 mm), and a zone of subsurface corrosion attack occurred to depths of about 0.002 inch (0.050 mm). The surfaces of the René 41 blades were much smoother and had less depth of penetration than either of the stainless steel blades.

18

(a) Pretest, 316 stainless-steel blade 9 before machining outside diameter.
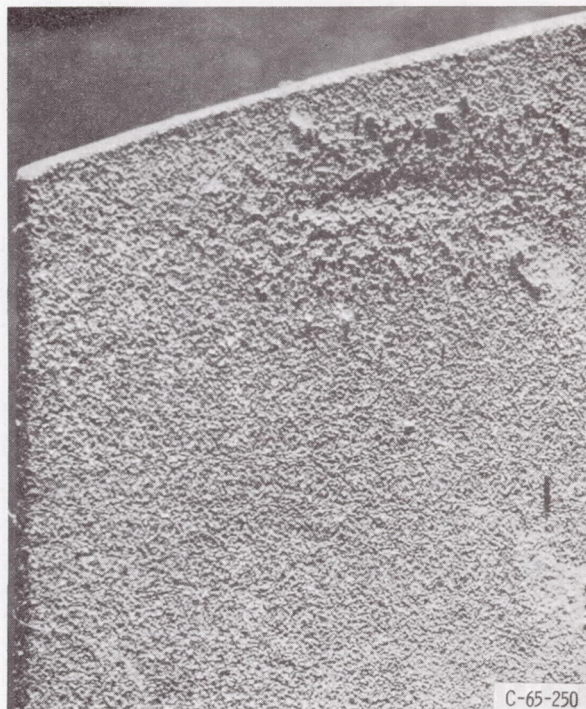
(b) Post-test, 316 stainless-steel blade 9.
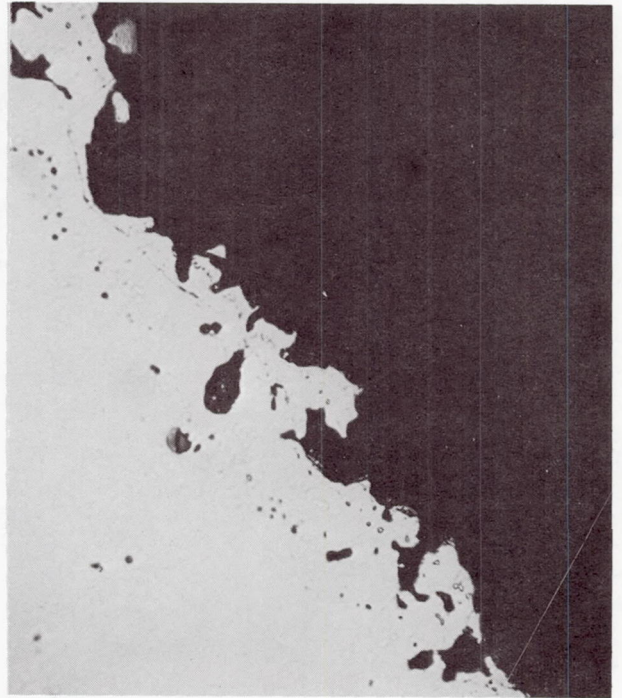
(c) Post-test, 318 stainless-steel blade 1.
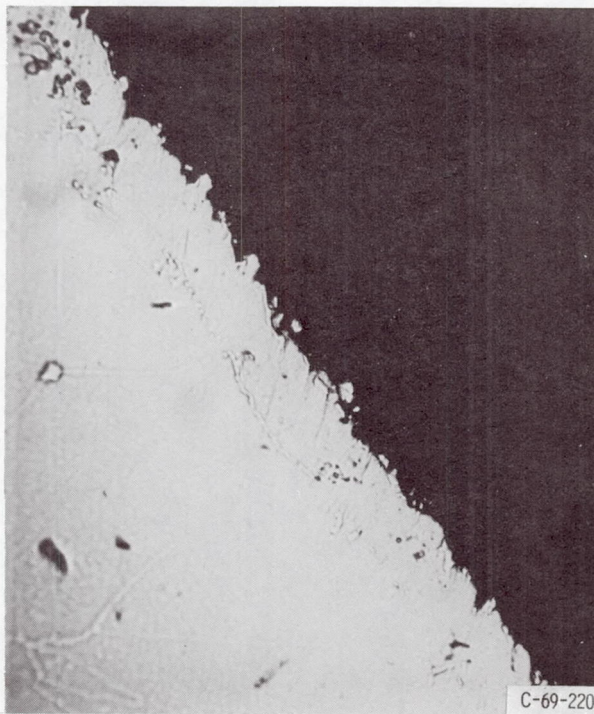
(d) Post-test, René 41 blade 8.

Figure 10. – Enlarged views of inlet tip suction surfaces of blades. (White areas are residual sodium oxide.)

19

(a) Blade 0, 316 stainless steel; pressure surface near tip. .

(b) Blade 1, 318 stainless steel; suction surface.

(c) Blade 2, René 41; suction surface.

Figure 11. - Post-test photomicrographs of section through blade showing surface profile.

# SUMMARY OF RESULTS

A study was conducted to determine long-term cavitation-damage characteristics for a low-head-rise axial-flow pump operated in high-temperature liquid sodium. Blades of different materials were used in the test rotor to evaluate the relative cavitation-damage resistance of the three representative blade materials (316 and 318 stainless steel and René 41, a nickel-chromium-base superalloy). The 5.0-inch- (127-mm-) diameter axial-flow rotor was operated for 558 hours in liquid sodium at temperatures to $1500^{\circ}$ F (1089 K). The following experimental results were obtained:

1. Slight localized cavitation damage was observed on the rotor blades after a 200-hour cavitation endurance test in $1500^{\circ}$ F (1089 K) sodium at a constant blade-tip speed of 75.5 feet per second (23.0 m/sec) and a constant suction specific speed of 6500. The cavitation damage was concentrated near the tip leading edge of the suction surface and extended back about 0.25 inch (6.4 mm) from the leading edge. The tip vortex cavitation formation did not cross the channel to cause damage to the pressure surface of the following blade.

2. The René 41 blades sustained less cavitation damage than either the 316 or the 318 stainless-steel blades. These results were confirmed by other investigators who tested materials in liquid sodium with a magnetostrictive device.

3. Roughening of the blade surface, which occurred for the three materials studied, was attributed to corrosion attack by the sodium.

4. Cavitation performance tests in $1500^{\circ}$ F (1089 K) sodium indicated that an initial dropoff in the pump total head-rise coefficient occurred at a constant value of suction specific speed of about 6000 for the three flow coefficients.

5. Satisfactory operation of the sodium pump, instrumentation, and test facility was obtained throughout the range of operating parameters.

Lewis Research Center,
    National Aeronautics and Space Administration,
        Cleveland, Ohio, January 6, 1969,
            128-31-32-12-22.

# APPENDIX - SYMBOLS

c      blade chord length, ft; m

D      blade diffusion factor, $1 - \dfrac{V_2'}{V_1'} + \dfrac{V_{2\theta}' - V_{1\theta}'}{2\sigma V_1'}$

g      gravitational constant, 32.2 ft/sec$^2$; 9.83 m/sec$^2$

H      total head, $P/\rho$, ft; m

$\Delta$H      pump total head rise, $H_2 - H_1$, ft; m

$H_{sv}$      net positive suction head, $H_1 - h_v$, ft; m

$h_v$      vapor head, ft; m

i      incidence angle (angle between direction of inlet flow relative to rotor and tangent to blade mean camber line at leading edge), $\beta_1' - \kappa_1$, deg

N      rotative speed, rpm

P      total pressure, psia; N/m$^2$ abs

p      static pressure, psia; N/m$^2$ abs

Q      flow rate, gal/min; cu m/sec

$S_s$      suction specific speed, $N\sqrt{Q} \Big/ \left(H_{sv}\right)^{0.75}$

s      blade tangential spacing, ft; m

U      rotor tangential velocity, ft/sec; m/sec

V      fluid velocity, ft/sec; m/sec

$\beta'$      flow angle (angle between direction of flow relative to rotor and axial direction), deg

$\delta$      deviation angle (angle between outlet flow direction relative to rotor and tangent to blade mean camber line at trailing edge), $\beta_2' - \kappa_2$, deg

$\kappa$      blade angle (angle between tangent to blade mean camber line at leading or trailing edge and axial direction), deg

$\rho$      fluid density, (lb)(sec$^2$)/ft$^4$; (N)(sec$^2$)/m$^4$

$\sigma$      blade solidity, c/s

$\varphi$      flow coefficient, $V_1/U_t$

$\psi$      head-rise coefficient, $g\Delta H/U_t^2$

Subscripts:

h      hub

t       tip

z      axial direction

$\theta$      tangential direction

1      pump inlet

2      pump outlet

Superscript:

'      relative to rotor

# REFERENCES

1. Smith, P. G.; DeVan, J. H.; and Grindell, A. G.: Cavitation Damage to Centrifugal Pump Impellers During Operation with Liquid Metals and Molten Salt at 1050-1400° F. Paper 62-HYD -2, ASME, May 1962.

2. Wood, G. M.: Cavitation Testing Techniques for High-Temperature Liquid Metal Systems. ASME Symposium on Cavitation Research Facilities and Techniques, Philadelphia, Pa., May 18-20, 1964, pp. 165-174.

3. Kulp, Robert S.; and Altieri, James V.: Cavitation Damage of Mechanical Pump Impellers Operating in Liquid Metal Space Power Loops. NASA CR-165, 1965.

4. Grennan, C. W.; and Lewis, R. A.: Cavitation Damage in a Liquid-Mercury Centrifugal Pump. Paper 63-WA-215, ASME, Nov. 1963.

5. Hartmann, Melvin J.; and Soltis, Richard F.: Observation of Cavitation in a Low Hub-Tip Ratio Axial-Flow Pump. Paper 60-HYD-14, ASME, Jan. 1960.

6. Young, Stanley G.; and Johnston, James R.: Accelerated Cavitation Damage of Steels and Superalloys in Liquid Metals. NASA TN D-3426, 1966.

7. Ross, C. C.; and Banerian, Gordon: Some Aspects of High-Suction Specific-Speed Pump Inducers. Trans. ASME, vol. 78, no. 8, Nov. 1956, pp. 1715-1721.

8. Crouse, James E.; Montgomery, John C.; and Soltis, Richard F.: Investigation of the Performance of an Axial-Flow-Pump Stage Designed by the Blade-Element Theory- Design and Overall Performance. NASA TN D-591, 1961.

9. Johnsen, Irving A.; and Bullock, Robert O., eds: Aerodynamic Design of Axial-Flow Compressors. NASA SP-36, 1965.

10. Eisenberg, P.; Preiser, H. S.; and Thiruvengadam, A.: On the Mechanisms of Cavitation Damage and Methods of Protection. Presented at the Society of Naval Architects and Marine Engineers Annual Meeting, Nov. 11-12, 1965.

11. Weiss, V.; and Sessler, J. G., eds: Aerospace Structural Metals Handbook. Syracuse Univ. Press, 1963.

12. Anon.: Stainless Steel Handbook. Allegheny Ludlum Steel Corp, 1951.